Applied Science and Innovative Research
ISSN 2474-4972 (Print) ISSN 2474-4980 (Online)
Vol. 9, No. 1, 2025
www.scholink.org/ojs/index.php/asir

Original Paper

Simulation Analysis of Keyway Shaft Cutting Based on Low Frequency Axial Vibration

Ningchao Zhang[1], Xufei Wang[1,2], Zhiqiang Xie[1] & Tongjiang Duan[3]

[1] School of Mechanical Engineering, Shaanxi University of Technology, Shaanxi hanzhong 72300, China

[2] Key Laboratory of Industrial Automation, Shaanxi Province, Shaanxi hanzhong 72300, China

[3] Wafangdian Bearing Group Corp., LTD., Liaoning Province, Wafangdian 116300, China

Corresponding Author: Xufei Wang, E-mail: wxf@snut.edu.cn.

Abstract

Low-frequency axial vibration cutting technology has advantages in reducing tool wear and improving processing surface quality, but further research is needed on this technology. This paper studies the influence of cutting parameters on the surface of keyway shaft processed by low-frequency axial vibration technology. Firstly, a two-dimensional simulation model of low-frequency axial vibration cutting of workpieces is established. Secondly, the range of the influence of vibration amplitude and tool rake angle on cutting performance is determined respectively. Then, a four-factor three-level orthogonal experiment is designed using vibration amplitude and frequency, tool rake angle, and relief angle. The results show that the optimal combination of the four factors is vibration amplitude of 1.0mm, vibration frequency of 50Hz, tool rake angle of 20°, and relief angle of 20°. Finally, through range analysis, it is determined that the influence of the four factors on cutting performance is in the following order: vibration amplitude, vibration frequency, tool rake angle, and relief angle. This simulation analysis can provide a reference basis for low-frequency axial vibration cutting of shaft-like parts.

Keywords

Low-frequency axial vibration, cutting, Shaft-like parts, finite element, orthogonal experiment

1. Introduction

Metal cutting is one of the fundamental and essential methods for removing excess metal or material allowance in part production. However, traditional cutting methods often face a series of challenges during the machining process, such as tool wear, poor surface quality, and difficulties in chip evacuation. These issues not only affect machining efficiency but also increase production costs and time. To overcome these obstacles and improve machining efficiency and quality, new cutting technologies are continuously being researched and developed.

Low-frequency axial vibration cutting technology has emerged as an effective solution to address the aforementioned problems. By introducing low-frequency vibrations during the cutting process, this technology creates periodic changes in the relative motion between the tool and the workpiece, significantly improving the distribution of cutting forces, reducing tool wear, optimizing chip morphology, and enhancing surface quality. Additionally, low-frequency axial vibration cutting technology excels in reducing chip accumulation and optimizing chip evacuation, which is particularly important for machining parts with complex shapes and high hardness materials. Previously, scholars both domestically and internationally have conducted extensive research on low-frequency axial vibration cutting. For instance, Yukio Takahashi and colleagues conducted in-depth predictive analysis on tool wear under low-frequency vibration cutting conditions; Nakamura S proposed a cutting tool specifically designed for low-frequency vibration cutting, elucidating its impact on surface roughness and roundness; Bai Xiaofan et al. studied the influence of axial low-frequency vibration-assisted drilling on feed force during cortical bone drilling; Yo K et al. focused on the field of low-frequency vibration cutting, exploring how phase difference φ can suppress chatter vibrations while ensuring that the material removal rate does not decrease ; furthermore, Kamada Y et al. experimentally investigated the periodic fluctuations of residual stress during the workpiece rotation phase in low-frequency vibration cutting; Akihito M et al. conducted tool wear experiments on the external cylindrical surfaces of shaft parts using a low-frequency axial turning machine. These studies on low-frequency axial vibration cutting primarily focused on vibration parameter optimization, tool wear, cutting mechanism analysis, and machining effect evaluation, but there has been no research on its application in shaft part machining.

Surface machining of shaft parts is typically carried out using methods such as turning, slotting, broaching, and grinding, which are characterized by low production efficiency, high energy consumption, and high machining costs. This paper investigates the process of machining spline shaft surfaces using low-frequency axial vibration cutting, with a focus on the influence of axial vibration cutting parameters on cutting force and temperature.

2. The Low-frequency Vibration Cutting Model was Established

2.1 Mechanical Model Building

Vibration cutting is to force the tool to vibrate the workpiece with a certain amplitude and frequency during the cutting process, and it is a new type of pulse cutting processing method. Let the forced vibration of the tool at the time of vibration be a simple harmonic vibration that does not attenuate, which is represented by Eq. (1).

$$x = A\,sin(wt + \phi_0) \tag{1}$$

x——Tool displacement;

A——The amplitude of tool vibration;

w——The angular frequency of the tool vibration, $w = 2\pi f$;

f——Tool vibration frequency;

t——Time;

ϕ_0——The initial phase of tool vibration.

The speed at which the tool vibrates is expressed as Equation 2.

$$v_t = \frac{\mathrm{d}x}{\mathrm{d}t} = Aw\, cos(w_t + \phi_0) \tag{2}$$

The acceleration of the tool vibration is expressed as Equation 3.

$$a_T = \frac{\mathrm{d}v_T}{\mathrm{d}t} = -Aw^2\, sin(wt + \phi_0) \tag{3}$$

From equations (2) and (3), it can be seen that the magnitude and direction of the tool speed are changing during vibration cutting, and the maximum value of the tool vibration speed ν_t is ν_t=Aw, if the cutting speed is greater than or equal to the maximum speed of tool vibration, that is, ν_t≥Aw, there will be no process of separation between rake face and chip. cause

$$k = \frac{v_w}{wA} \tag{4}$$

Weigh k as the velocity coefficient. When k≥1, the rake face of the tool is not separated from the chip, which is a non-separating type of vibration cutting; When k≤1, the rake face of the tool will be separated from the chip.

Therefore, the mechanical-dynamic equation of motion for vibratory cutting is proposed:

$$m\frac{\mathrm{d}^2x_2}{\mathrm{d}t^2} + C_0\frac{\mathrm{d}x_z}{\mathrm{d}t} + k_0x_2 = P_2(t) \tag{5}$$

where: x_2 - the displacement of the workpiece in the horizontal direction; P_2 (t) – the cutting resistance of the pulsed waveform of the vibratory cut, the Fourier series expansion is:

$$P_2(t) = \frac{tc}{T}P_0 + \frac{2P_0}{\pi}\sum_{n=1}^{\infty}\frac{1}{n}sin\frac{n^tc}{T}\pi c\, cos\, nwt \tag{6}$$

Where: tc - cutting time in a cycle; T – vibration period.

Therefore, according to the cutting theory, the main cutting force in the vibration cutting process will be greatly reduced with the reduction of the cutting force, which is the mechanism that vibration cutting can significantly reduce the main cutting force. The schematic model of the low-frequency axial vibration cutting tip trajectory is shown in Figure 1, while the workpiece moves forward along the x direction with velocity v, the tool does low-frequency reciprocating vibration in the x-direction with the vibration amplitude A and frequency f. When the tip of the tool comes into contact with the workpiece, it begins to enter the cutting, and the workpiece material undergoes shear deformation to form chips.

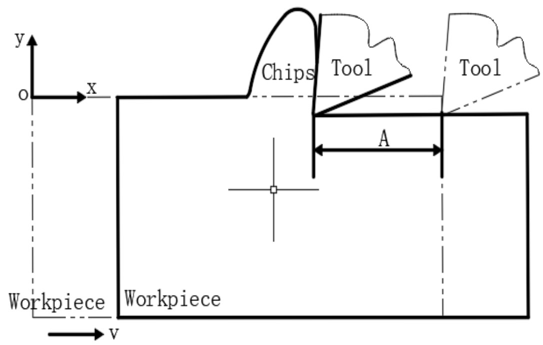

Figure 1. Schematic Diagram of Cutting Tool Tip Trajectory with Low-frequency Axial Vibration

2.2 Cutting Deformation Zone Division

The metal cutting process is complex, and the tool acts directly on the workpiece, causing the geometry of the workpiece to change. It is very difficult to comprehensively, meticulously and completely describe and characterize the process in a comprehensive, detailed and complete manner due to the geometry, mechanics, tribology, metal microstructure, thermal, acoustic, chemical and even optical changes in the process of metal cutting. In the process of metal cutting, various elastic and plastic deformations of the workpiece under the action of the cutting force of the tool are collectively referred to as cutting deformation. According to the different stress-strain characteristics of each part of the cutting deformation zone, the demarcation area between the cut layer and the chip is generated, which is the I.-basic deformation zone. II.—Knife-chip contact deformation zone; III.—Tool-work contact deformation zone, cutting deformation zone division as shown in Figure 2.

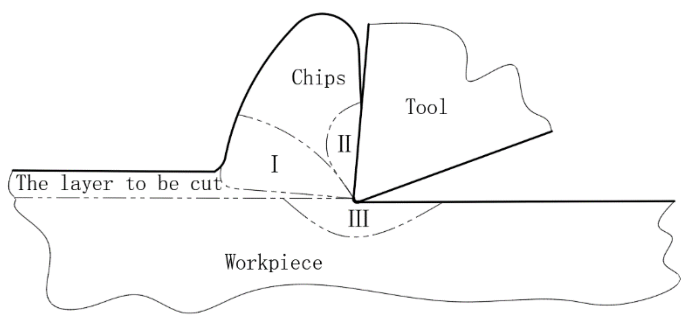

I—Basic deformation zone; II.—Knife-chip contact deformation zone; III.—Tool-worker contact deformation zone

Figure 2. Division of the Cutting Deformation Zone

The basic deformation zone I is the part of the metal to be cut that flows out along the rake face through the deformation of the cutting layer and the chip separation zone. The cutter-chip contact deformation zone II is the part of the chip that flows out along the rake face after the shear slip deformation of the basic deformation zone, and the material at the bottom of the chip is further shear-slip deformed due to the strong friction between the rake face and the rake face of the tool due to the extrusion of the rake face. The tool-work contact deformation zone III is that after the cutting layer is broken and separated from the workpiece matrix near the cutting edge, the upper material is deformed into chips by the I. and II zones, and the lower material will form the machined surface on the workpiece after the knife-work contact zone is ironed on the rake face of the tool.

3. Simulation of Low-frequency Vibration Cutting Processes

3.1 Establish a Finite Element Model

In order to study the process method of low-frequency axial vibration cutting technology in the machining of shaft parts, and to study the role and influence of tool geometric parameters and cutting parameters in vibration cutting, the cutting model of shaft parts represented by spline shafts in annular tool machining was constructed. Since the 3D model of the annular tool axial vibration cutting spline shaft has a symmetrical structure of the center of the tool and the workpiece, this facilitates the simulation calculations. We simplified the ring tool and splined shaft from 3D to 2D for cutting simulation, and the simplified process is shown in Figure 3. Figure 3(a) shows a three-dimensional model of a circular cutter machining a splined shaft by axial vibration cutting; Figure 3(b) is a half-sectioned 3D model showing the internal tooth structure of the tool and spline shaft; Figure 3(c) shows a simplified 2D model showing the axial cutting of a splined shaft with a single tooth. This simplified 2D cutting model facilitates further analysis of the low-frequency axial vibration cutting process.

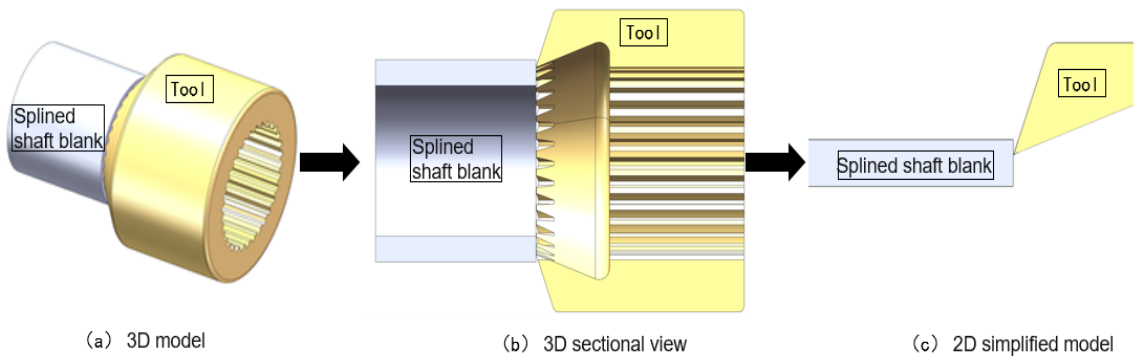

Figure 3. Schematic Diagram of the Simplification Process of the Spline Shaft Cutting Model

Thirdwave-advantEdge software was used for cutting modeling and simulation calculation, and in order to facilitate observation, the direction and position of the tool in the simplified model were adjusted, and the two-dimensional cutting finite element model as shown in Figure 4 was established.

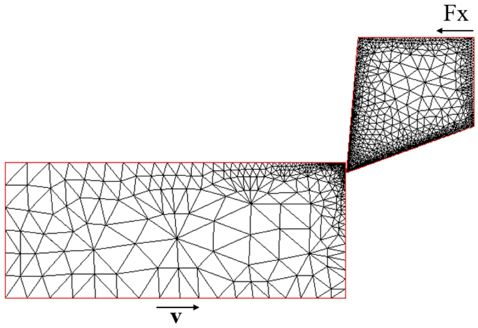

v—the speed at which the workpiece moves; Fx—the axial force in the X direction of the tool

Figure 4. 2D Cutting Finite Element Model

The length and width of the workpiece shown in Figure 4 are 5.0mm×2.0mm, the finite element meshing is carried out on the tool and the workpiece with software, the mesh adopts a four-node linear tetrahedral element, and the part that participates in the cutting on the rake face, the rake face and the workpiece is meshed for mesh refinement, and the maximum mesh size is 0.10mm and the minimum mesh size is 0.02mm in the finite element model. The cutting speed is set to 1200mm/min and the ambient temperature is set to 20 ℃. The workpiece material is made of 45 steel, and the tool material is diamond cutter.

3.2 Univariate Experimental Analysis

Only a fraction of the energy done by the cutting force is stored in the workpiece and chips as deformation energy, and most of this will be converted into thermal energy, i.e., the heat of cutting, which produces a very high cutting temperature in the cutting zone. Cutting forces and cutting temperatures not only play a decisive role in tool durability, machining accuracy, and the integrity of machined surfaces, but also have a significant impact on the entire process system such as machine tools, tools, and fixtures. Tong Fuqiang et al. pointed out in their paper that with the increase of vibration frequency f and the decrease of cutting speed, the more obvious the vibration cutting effect, the better the cutting effect. Peng Baoying et al. found that the continuous increase of the tool rear angle has a relatively small impact on the horizontal cutting force Fx, but has a relatively large impact on the vertical cutting force Fy. However, the influence of amplitude amplitude and tool rake angle on cutting force and cutting temperature is insufficient, so this paper first uses the single factor change method to study the influence of vibration amplitude and tool rake angle on cutting force and cutting temperature.

3.2.1 Effect of Vibration Amplitude on Low-frequency Vibration Cutting

The parameters of the vibration amplitude single-factor experiment were set to the cutting depth of 0.1mm, the rake angle of the tool 15°, the rear angle of the tool 10°, the radius of the arc of the tool tip of 0.05mm, the frequency of 40Hz, the vibration amplitude value was set from the minimum value of 0.4mm, and the amplitude step was 0.2mm, and a total of 7 groups of experiments were designed.

Through simulation calculations, the results of the average cutting force and cutting temperature of seven groups are shown in Table 1.

Table 1. Experimental Scheme and Results of Single Factor on Vibration Amplitude

Experiment number	Amplitude Ax/mm	Force Fx/N	Temperature T/℃
1	0.4	120.8	74.9
2	0.6	105.1	78.1
3	0.8	92.4	73.7
4	1.0	80.0	74.2
5	1.2	79.5	83.9
6	1.4	66.0	79.3
7	1.6	65.5	83.5

According to the simulation experiments in Table 1, the influence curve of vibration amplitude on cutting force and temperature is plotted as shown in Figure 5. It can be seen from the cutting force curve that the cutting force gradually decreases with the increase of vibration amplitude; From the perspective of the cutting temperature curve, with the increase of vibration amplitude, the average cutting temperature is generally kept in the range of 70 ℃ ~ 90 ℃, so that it can be concluded that although the average cutting force decreases with the increase of cutting amplitude, the maximum temperature will gradually increase with the increase of amplitude.

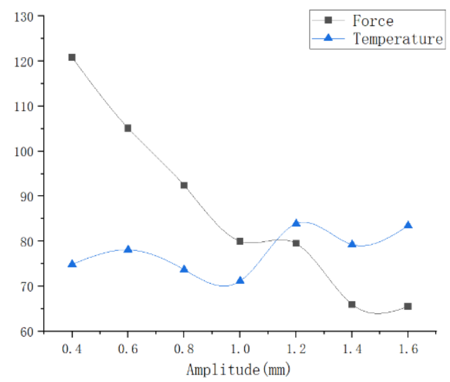

Figure 5. Influence Curve of Vibration Amplitude on Cutting Force and Temperature

According to the simulation results obtained from the above experiments, the temperature distribution contours corresponding to the amplitudes of the four groups are listed as shown in Figure 6. Among them, the highest temperature occurs at the chip and the rake face where the tool tip is in contact with the chip, that is, the knife-chip contact deformation zone, and the second temperature change occurs in the tool-chip contact deformation zone. As the amplitude increases, so does the maximum temperature.

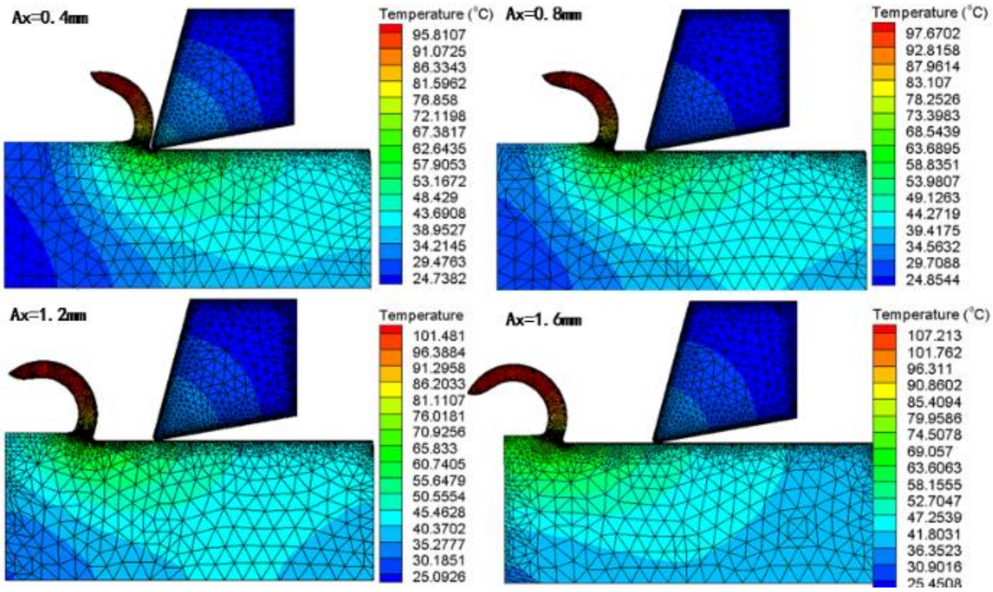

Figure 6. Temperature Distribution Contour Map Influenced by Different Vibration Amplitudes

3.2.2 The Effect of Tool Rake Angle on Low-frequency Vibration Cutting

The parameters of the single factor test of the rake angle of the tool were set to the cutting depth of 0.1mm, the vibration amplitude of 1.0mm, the rear angle of the tool 10°, the radius of the arc of the tip of the tool 0.05mm, the frequency of 40Hz, the rake angle of the tool from 5°, the step length of 2°~5°, a total of 6 groups of experiments. Through simulation calculation, the results of six groups of average cutting force and cutting temperature are shown in Table 2.

Table 2. Experimental Scheme and Results of Single Factor on Cutting Tool Rake Angle

Experiment number	Tool rake angle / °	Force/N	Temperature/°C
1	5	120.8	74.9
2	8	105.1	78.1
3	10	92.4	73.7
4	12	80.0	74.2
5	15	79.5	83.9
6	20	66.0	79.3

According to the simulation experiments in Table 2, the influence curve of the tool rake angle on the cutting force and temperature is plotted as shown in Figure 7. It can be seen from the cutting force curve and temperature curve that the influence of the tool rake angle on the cutting is mainly reflected in the average cutting force, the average cutting force shows a downward trend with the gradual increase of the tool rake angle, and the average temperature also has a slow downward trend.

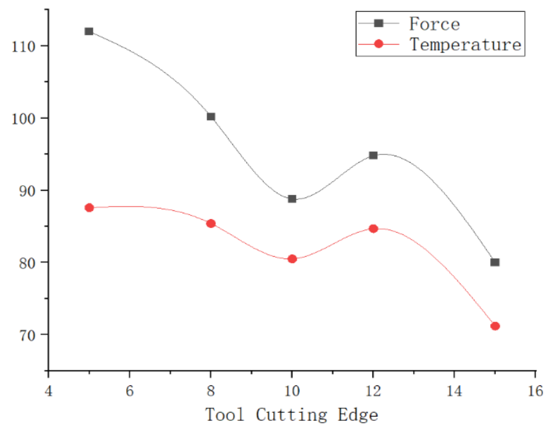

Figure 7. Influence Curve of Cutting Tool Rake Angle on Cutting Force and Temperature

According to the simulation results obtained from the above experiments, the temperature distribution contour corresponding to the rake angles of the four groups of tools is listed as shown in Figure 8. The maximum temperature occurs in the chip area and decreases as the rake angle increases.

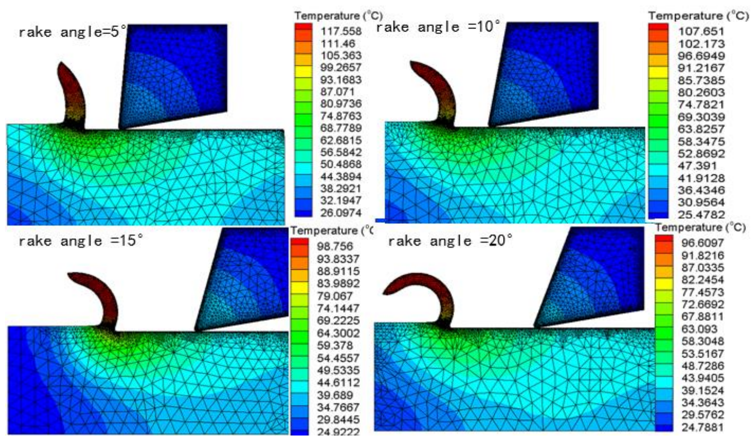

Figure 8. Temperature Contour Map at Different Cutting Tool Rake Angles

4. Orthogonal Experiments

4.1 Protocol Design

In order to find out the influence trend of multiple factors in low-frequency axial vibration cutting, the orthogonal experimental method was carried out on 45 steel materials. Based on the finite element simulation model shown in Figure 3, the cutting speed is set to 1.2 m/min, the cutting depth is 0.1 mm, and the arc radius of the cutting edge is 0.05 mm. The orthogonal experimental scheme is designed as four factors and three levels, the four factors are the vibration frequency, vibration amplitude, tool rake angle and tool back angle, and the level refers to the influence of the average temperature of each parameter in the single factor experiment, and the orthogonal experimental level table shown in Table 3 is obtained. For the cutting frequency, because the frequency has a great influence on the cutting force and cutting temperature, the three values below the middle under the concept of low frequency are adopted. In the simulation experiment of the influence of vibration amplitude on single factors, the values from small to large according to the average temperature are from 1.0mm<0.8mm<0.4mm. In the simulation experiment of the influence of tool rake angle on single factor, the values from small to large according to the average temperature are from 20 °< 15 °<10 °. In the simulation experiment of the influence of the tool rear angle on the single factor, according to the 8 °, 10 ° and 20 mentioned in the experiment, the orthogonal experimental level table obtained is shown in Table 3.

Table 3. Orthogonal Experimental Scheme Level for 45 Steel

Factor / Level	Amplitude A (Ax/mm)	Frequency B (F/Hz)	Tool rake angle C (a/deg)	Tool trailing angle D (b/deg)
1	1.0	50	20	20
2	0.8	40	15	10
3	0.4	30	10	8

4.2 Experimental Results and Analysis

The simulation experiments are carried out according to the orthogonal experimental scheme, and the experimental results are shown in Table 4.

Table 4. Orthogonal Experimental Scheme and Results for 45 Steel

Factor / Number	Amplitude A(Ax/mm)	Frequency B(F/Hz)	Tool rake angle C(a/deg)	Tool trailing angle D(b/deg)	Force (Fx/N)	Temperatu re (°C)
1	1.0	50	20	20	72.2	83.8
2	1.0	40	15	10	79.2	79.7
3	1.0	30	10	8	106.6	83.0
4	0.8	50	15	8	87.8	80.7
5	0.8	40	10	20	102.8	85.3
6	0.8	30	20	10	106.0	80.7
7	0.4	50	10	10	147.4	83.8
8	0.4	40	20	8	113.2	73.3
9	0.4	30	15	20	169.3	86.4

According to the experimental results in Table 4, the orthogonal experimental cutting force and cutting temperature curves are plotted, as shown in Figure 9.

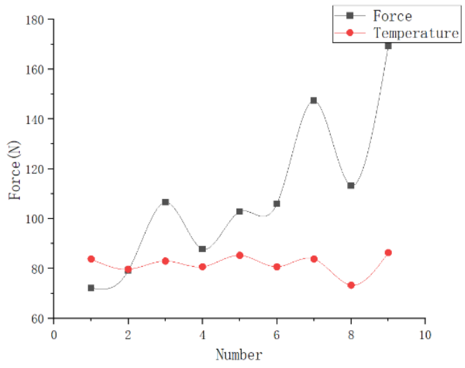

Figure 9. Influence Curves of Cutting Force and Temperature in Orthogonal Experiments

As can be seen from Figure 9, the average cutting force of experiment 1 is the lowest at 72.2 N, and the highest cutting force is 169.3 N in experiment 9. As can be seen from the temperature line, the cutting temperature of experiment 8 was the lowest at 73.3 ℃, and the highest temperature was 86.4 ℃ in experiment 9. Although the difference in the average cutting force is 97.1 N under different cutting parameters, the range of the average temperature is much smaller than that of the cutting force, and the variation is only 13.1 ℃.

According to Table 4 and Figure 9, it can be seen that the optimal horizontal combination is the vibration amplitude value of 1.0mm, the vibration frequency of 50Hz, the rake angle of the tool 20 °, and the rear angle of the tool 20 °, and the temperature contour of the optimal horizontal combination simulation is shown in Figure 10. In the common axial cutting simulation, the rake angle and rake angle of the tool are 20 °, the corresponding cutting force is 394.9N, and the cutting temperature is 84.4 ℃. Compared with ordinary cutting, the cutting force of low-frequency axial vibration cutting is reduced by 81.7%. Through orthogonal experimental analysis, simulation analysis of low-frequency axial vibration machining and comparison of the characteristics of vibration cutting, it is found that the introduction of low-frequency axial vibration in annular axial vibration cutting can realize high-precision and high-efficiency cutting of shaft parts represented by splined shafts.

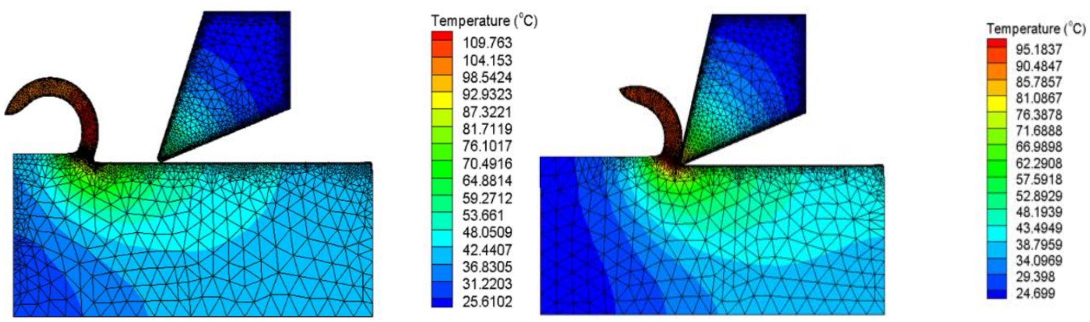

(a) Optimal level combination (b) General cutting simulation

Figure 10. Comparison Map of Cutting Simulation Temperature Contours

Published by SCHOLINK INC.

According to the orthogonal test results, the range analysis can be obtained as shown in Table 7, which can judge the changes of each level factor in different indicators, compare the influence degree of different factors, and determine the optimal level combination. The average value of the principal cutting force corresponding to each test at the same level is recorded as $\overline{K_i}$(i=1,2,3). The range R is the difference between the maximum and minimum values in $\overline{K_i}$:

$$Rj = \max(\overline{K_{ij}}) - \min(\overline{K_{ij}}) \tag{7}$$

Wherein: j--the corresponding values under the four factors of A, B, C, and D;

The higher the value of R, the higher the influence of this factor, and the smaller the value of R, the lower the influence of this factor. Therefore, it can be considered that according to the R value, the primary and secondary positions of multiple factors in the test can be determined.

Table 5. Range Analysis of Orthogonal Experiments

Index	Amplitude A(Ax/mm)	Frequency B (F/Hz)	Tool rake angle C(a/deg)	Tool trailing angled D(b/deg)
K_1	86.0	102.467	97.1	114.8
K_2	98.9	98.4	112.1	110.9
K_3	143.3	127.3	119.0	102.5
R	57.3	28.9	21.8	12.2

According to the value of R in Table 5, the vibration amplitude Ax has the greatest influence on the cutting force, and the vibration frequency F and the tool rake angle have the second influence on the cutting force, so in considering the influence on the cutting force, the vibration amplitude is selected first, and then the vibration frequency is considered. In the tool parameters, the rake angle of the tool is selected first, so that the size of the cutting force can be reasonably reduced.

5. Conclusion

In order to explore the process method of low-frequency axial vibration cutting technology for shaft parts, this paper studies the influence of optimal vibration cutting parameters and tool geometric parameters on cutting force and cutting temperature by simplifying the simulation analysis of low-frequency axial vibration cutting shaft workpieces.

By using the Thirdwave-advantEdge software, a two-dimensional finite element model of low-frequency axial vibration cutting was established, and the 45 steel material was simulated by using diamond tools. Firstly, the influence of vibration parameters and tool parameters on the cutting effect under low-frequency axial vibration cutting was analyzed by single factor experiment, and it was concluded that the cutting force gradually decreased with the increase of vibration amplitude and tool rake angle. Secondly, based on the results of the single-factor experiment, four factors were selected:

vibration frequency, vibration amplitude, tool rake angle and tool back angle, and the four-factor three-level orthogonal test was carried out. The analysis shows that a set of optimal horizontal cutting parameters are vibration amplitude of 1.0mm, vibration frequency of 50Hz, tool rake angle of 20 ° and tool rear angle of 20 °, and the low-frequency axial vibration cutting force under the optimal horizontal parameters is reduced by 81.7% compared with ordinary cutting. In addition, through the range analysis, it is concluded that the four factors have a large to small influence on the cutting performance, which are vibration amplitude, vibration frequency, tool rake angle and rear angle.

References

Akihito, M., Ayako, K., Seiko, K., et al. Influence on surface characteristics generated in Low Frequency Vibration Cutting. *The Proceedings of Mechanical Engineering Congress, Japan*, 2018, *2018*(0), S1320203-S1320203.

Bai Wei. *Experimental study on vibration-assisted cutting mechanism and machinability of typical difficult-to-machine materials*. Huazhong University of Science and Technology, 2018.

Bai, X., Liu, Z., & Liu, Y. Experiments and Analyses of Effects of Axial Low-frequency Vibration on Feed Forces of Cortical Bone Drilling. *China Mechanical Engineering*, 2023, *34*(20), 2411.

Feasibility study of high-speed ultrasonic vibration cutting titanium alloy. *Journal of Mechanical Engineering*, 2017, *53*(19), 120-127.

Han Qingkai, Hao Jianshan, & Wen Bangchun. Vibration utilization in metal material processing. *China Mechanical Engineering*, 2001, (05), 115-118+9.

High quality and efficient ultrasonic vibration cutting of titanium alloys. *Journal of Mechanical Engineering*, 2021, *57*(5), 133-147.

Kamada, Y., & Sasahara, H. Residual stress fluctuates periodically via the workpiece rotation phase during low frequency vibration cutting. *Precision Engineering*,*72*, 583–594.

Liu Yangwen, Zhang Ying, & Ji Zhongchao. CAE analysis and process parameter optimization of cold extrusion forming of automotive spline shaft. *Mould Technology*. 2018, No.003.

Mohammad. The effect of chip breaker geometry on chip shape, bending moment, and cutting force: FE analysis and experimental study. *International Journal of Advanced Manufacturing Technology*, 2015, *78*(5-8), 917-925.

Peng Baoying, Xu Dong, & Wang Pengjia. Simulation of the influence of tool material and angle on the cutting force of 7075-T6 aluminum alloy. *Tool technology*, 2023, *57*(12), 131-134.

Shi Tuanle, Liu Qianfeng, Kou Jingling, et al. Research on Ta-10W alloy material cutting technology. *Mechanical Engineering and Automation*, 2024, (04), 126-128.

Shogo, N., Kenichi, N., Kenji, O., et al. Tool design for low-frequency vibration cutting on surface property. *Frontiers in Manufacturing Technology*, 2023.

Sun Yuhan, Zhang Yijia, Yang Yanchao, et al. Research progress of ultrasonic elliptical vibration cutting of difficult-to-machine materials. *Manufacturing technology and machine tools*, 2024, (01), 100-107.

Tong Fuqiang, Zhang Feihu, Chen Guangjun, et al. Research on the mechanism of the influence of low-frequency vibration cutting on the machined surface. *Journal of Huazhong University of Science and Technology* (Natural Science Edition), *2007*(S1), 68-70.

Yo, K., Ayako, K., Kazuhiko, S., et al. Mechanism to suppress regenerative chatter vibration due to the effect of air-cutting and multiple regeneration during low frequency vibration cutting. *Precision Engineering*, 2022, 781-18.

Takahashi Yukio, Sato Akimasa, Fujita Haruto, et al. Prediction of Tool Wear in Low-Frequency Vibration Cutting. *Proceedings of the Academic Lecture Meeting of the Japan Society for Precision Engineering*, 2021, *2021S*(0), 202-203.